

Background Considerations for the $^2\text{H}(^7\text{Be},^3\text{H})^6\text{Be}$ Experimental Data Using the Phase Space Model

K. Y. CHAE*

Department of Physics, Sungkyunkwan University, Suwon 440-746, Korea

V. GUIMARÃES

Instituto de Física, Universidade de São Paulo, C.P. 66318, 05389-970 - São Paulo, SP, Brazil

(Received 22 August 2014, in final form 27 August 2014)

The $^2\text{H}(^7\text{Be},^3\text{H})^6\text{Be}$ reaction was measured at the Holifield Radioactive Ion Beam Facility of the Oak Ridge National Laboratory in 2004 to search for the resonances in the unbound ^6Be nucleus. The results showed, however, no resonance was evident in the experimental data, which implied that the direct transfer to ^6Be levels was not particularly strong compared to other reaction mechanisms that produced tritons in their exit channels. In the present work, theoretical calculations with background considerations are performed to better understand the cross-section data for the $^2\text{H}(^7\text{Be},^3\text{H})^6\text{Be}$ reaction using the phase space model.

PACS numbers: 24.10.Cn, 24.60.Gv, 25.40.Hs, 27.20.+n

Keywords: Radioactive ion beams, Inverse kinematics, Transfer reactions, Phase space model, Background considerations

DOI: 10.3938/jkps.65.1356

I. INTRODUCTION

Nuclear reactions often produce large numbers of light particles which come from nuclear reaction mechanisms other than the one originally desired. One example is the $^2\text{H}(^7\text{Be},^3\text{H})^6\text{Be}$ measurement performed at the Holifield Radioactive Ion Beam Facility (HRIBF) at the Oak Ridge National Laboratory (ORNL) in late 2004 [1], which is summarized in Section II. The purpose of that measurement was to search for resonances in the unbound ^6Be nucleus by detecting recoiling tritons. As summarized in the next section, however, the existence of a resonance was not evident in the experimental data, indicating that the direct transfer to ^6Be levels is not particularly strong compared to other reaction mechanisms. The upper limits on the $^7\text{Be}(d,t)^6\text{Be}$ reaction cross-section for hypothetical levels were set in Ref. [1], but further investigations are required to better understand the experimental data.

Background considerations might be useful in understanding the origin of the light particles (tritons in this case) other than direct (d,t) reaction mechanism. By estimating the theoretical cross sections of the reaction that can also produce tritons and by subtracting the calculated cross sections from observed triton energy spectra, one might reveal evidence of the resonances. Possible

mechanisms that can be used to understand the origin of tritons in the spectrum include the phase space model (PSM) [2] and the three-body continuum (sequential decay) [3,4]. In the current article, the PSM is adopted to explain the triton spectrum of the $^7\text{Be}(d,t)^6\text{Be}$ reaction measurements.

II. SUMMARY OF THE $^2\text{H}(^7\text{Be},^3\text{H})^6\text{Be}$ DATA

The experimental setup and the data shown in this section are taken and summarized from Ref. [1]. The $^7\text{Be}(d,t)^6\text{Be}$ reaction was measured in inverse kinematics at the HRIBF by utilizing a radioactive ^7Be ($t_{1/2} = 53.2$ days) beam at an energy of 100 MeV to search for resonances in the unbound ^6Be nucleus. The beam impinged on deuterated polyethylene $(\text{CD}_2)_n$ targets, and the recoiling tritons were detected by using a silicon detector array (SIDAR). The SIDAR was composed of six $\Delta E - E$ telescopes (100- and 500- μm thick) to identify incident charged particles. Each telescope was backed by a 300- μm -thick “veto” detector in order to reject ^3He particles that punched through the E layer. A total of 18 silicon strip detectors were used to form the array. Each detector was segmented into 16 annular strips, which enabled us to extract the angular distributions of the observed energy levels. The observed spectra of tritons obtained at 16 different angles, however, were rather featureless,

*E-mail: kchae@skku.edu; Fax: +82-31-290-7055

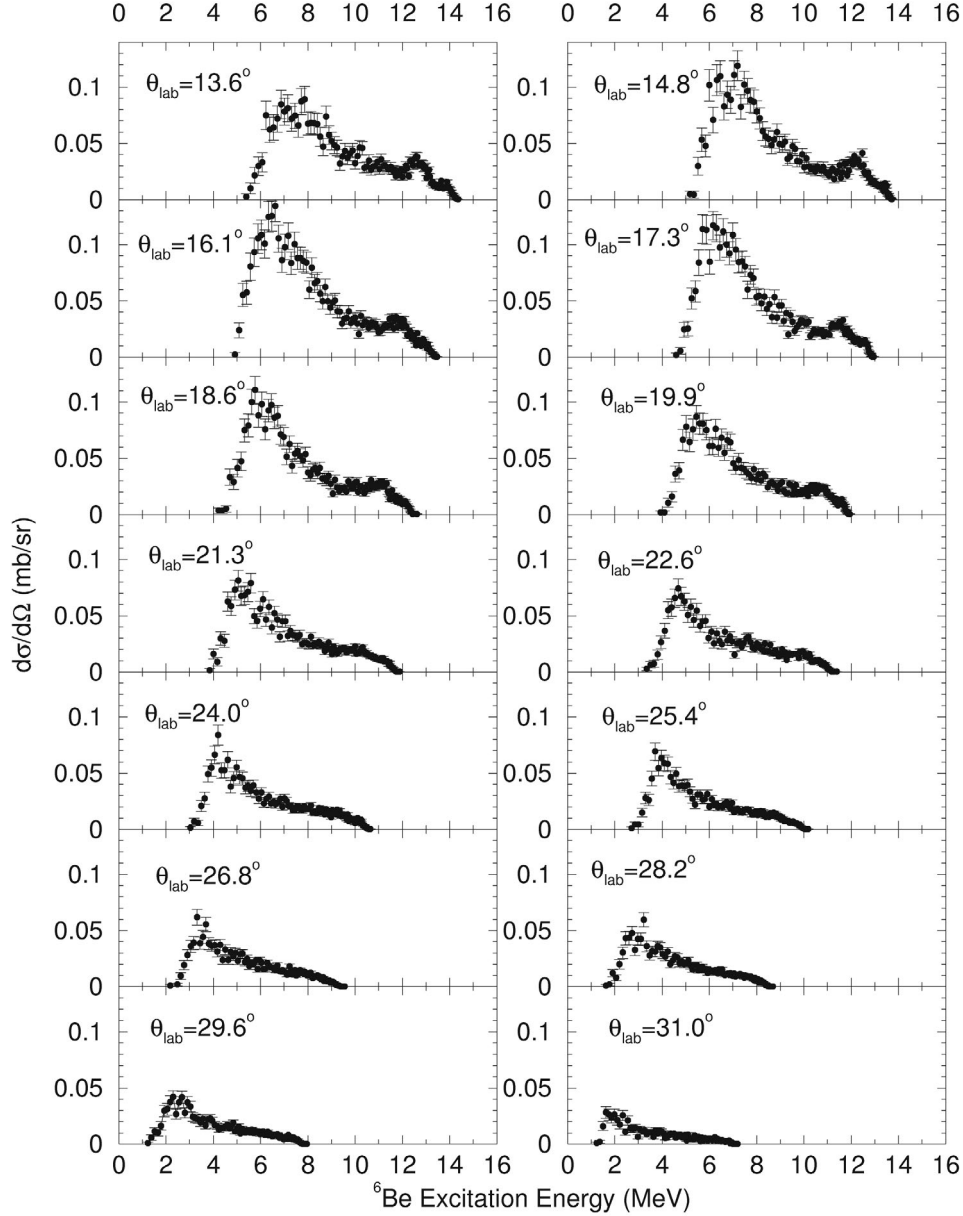


Fig. 1. Differential cross section as a function of ${}^6\text{Be}$ excitation energy. The figure is taken from Ref. [5].

indicating that reaction mechanisms other than direct transfer to ${}^6\text{Be}$ levels also produced tritons.

The differential cross-section of the ${}^2\text{H}({}^7\text{Be}, {}^3\text{H}){}^6\text{Be}$ reaction versus ${}^6\text{Be}$ excitation energy obtained at several SIDAR strips (angles) is plotted in Fig. 1. If any energy levels in the ${}^6\text{Be}$ nucleus were strongly populated through the ${}^7\text{Be}(d, t){}^6\text{Be}$ reaction, the figure should exhibit a peak at around the corresponding triton energy range. As shown in the figure, however, no ${}^6\text{Be}$ levels were evident. The peak-like structure at $E_x \sim 13$ MeV shown in the spectrum obtained at 13.6° is due to ${}^3\text{He}$ particles that punched through the “veto” detector.

Because no ${}^6\text{Be}$ levels were evident, a study of possible background mechanisms could be useful to better

understand the experimental data. In the present work, the PSM is introduced to estimate the triton’s energy distributions.

III. PHASE SPACE MODEL (PSM)

The PSM was originally developed by Enrico Fermi as a statistical method for computing high-energy collisions of protons with multiple production of particles [2]. In the case of nuclear collisions at very high energy, some π -mesons (pions) and anti-nucleons might be produced, which cannot be interpreted by using the conventional

perturbation theory. The general idea of the PSM is the following, which is a summary based on Ref. [2]:

When two nucleons collide with high energy in their center-of-mass system, the energy will be released in a relatively small region surrounding the two nucleons due to the pion field that surrounds the nucleons. Owing to the strong interactions of the pion field, this energy will then be rapidly distributed among the various degrees of freedom. In the PSM, the particles into which the energy has been transferred will be assumed to be emitted in all directions in their center-of-mass frame. The energy, charge, and momentum of the system should be conserved, of course. Furthermore, imagining that only the states that can be easily accessible from the initial state may attain statistical equilibrium is natural. The purpose of the PSM is, thus, computing statistically the probability of pion creation with a given energy distribution. As the wave function plays a central role in the Schrödinger picture, the phase-space distribution is the starting point in the phase-space picture of quantum mechanics [6].

If T_{if} is the matrix element for the transition from the initial state i to a final state f and w is the density of states, the first-order perturbation theory gives the cross section as

$$\sigma = \frac{2\pi}{\hbar} \frac{|T_{if}|^2}{|\text{flux}|} w. \quad (1)$$

Notice that only states that are allowed by conservations of energy and momentum should be considered [7]. When $|T_{if}|^2$ is not (or very slightly) dependent on the momenta and when a statistical equilibrium is reached, the PSM (sometimes called the statistical model) can be used. The first step is to replace $|T_{if}|^2$ with a mean constant value C as proposed by Fermi in Ref. [2].

In the PSM, there is only one adjustable parameter: the volume Ω , in which the energy of the two colliding nucleons is dumped. One can expect the order of Ω to be $\sim \hbar/\mu c$ because the strong pion field surrounding the nucleons extends to a distance of that order. μ is the mass of the pion in this notation. Therefore, the form of Ω is

$$\Omega = \Omega_0 A \quad (2)$$

$$= \frac{4\pi R^3}{3} A, \quad (3)$$

where R is the radius of the volume ($R = \hbar/\mu c = 1.4 \times 10^{-13}$ cm), and A is the Lorentz contraction ($A = 2Mc^2/W$, where M is the nucleon mass and W is the total energy of the two colliding nucleons). The term A is required only if the two interacting nucleons have relatively large energies. In these notations, the assumption of statistical equilibrium can be stated such that $|T_{if}|^2$ is proportional to the probability that all particles are confined inside Ω at the same time.

If there are n -bodies in the exit channel, the phase-space distribution for particle i in the center-of-mass sys-

tem can be written as [8]

$$P_i^{c.m.}(\mu, E, E') = C_n \sqrt{E'} (E_i^{\max} - E')^{\frac{3n}{2}-4}, \quad (4)$$

where E is the incident energy, E' is the energy of the product emitted with $\mu = \cos \theta_{cm}$, E_i^{\max} is the maximum possible energy for particle i in the center-of-mass frame, and C_n are normalization constants defined as follows:

$$C_3 = \frac{4}{\pi(E_i^{\max})^2}, \quad (5)$$

$$C_4 = \frac{105}{32(E_i^{\max})^{7/2}}, \quad (6)$$

$$C_5 = \frac{256}{14\pi(E_i^{\max})^5}. \quad (7)$$

In the laboratory system, the expression of the distribution becomes

$$P_i^{\text{lab}}(\mu, E, E') = C_n \sqrt{E'} \left[E_i^{\max} - (E^* + E' - 2\mu\sqrt{E^*E'}) \right]^{\frac{3n}{2}-4}, \quad (8)$$

where E^* is the energy of the center-of-mass motion in the laboratory. Notice that in this equation, E (incident energy), E' (outgoing energy), and $\mu = \cos \theta_{lab}$ are the values measured in the laboratory system. Here, the value of E_i^{\max} , a fraction of the energy available in the center-of-mass system, is given by

$$E_i^{\max} = \frac{M - m_i}{M} E_a, \quad (9)$$

where M is the total mass of the n -particles and E_a is the energy available in the center-of-mass system for one-step reactions ($E_a = E \frac{m_T}{m_p + m_T} + Q$).

IV. RESULTS AND DISCUSSION

In case of the ${}^7\text{Be} + d$ system, the following three exit channels can be considered by adopting the PSM described above:

$${}^7\text{Be} + d \Rightarrow \begin{cases} t + p + p + {}^4\text{He} & \text{(a)} \\ t + {}^3\text{He} + {}^3\text{He} & \text{(b)} \\ t + p + {}^5\text{Li} & \text{(c)}. \end{cases}$$

There are, of course, more channels that can produce tritons in their exit channels. Examples include ${}^3\text{Li} + t + t$ and ${}^4\text{Li} + t + d$. These channels are, however, not possible at the 100-MeV beam energy of ${}^7\text{Be}$ due to kinematics.

The PSM distributions for the three channels above were calculated with proper normalization factors of C_4 for the exit channel (a) and C_3 for the exit channels (b) and (c). The overall normalization factor is (*i.e.*, the factor required to fit experimental data), however, still undetermined. The calculated phase-space distributions

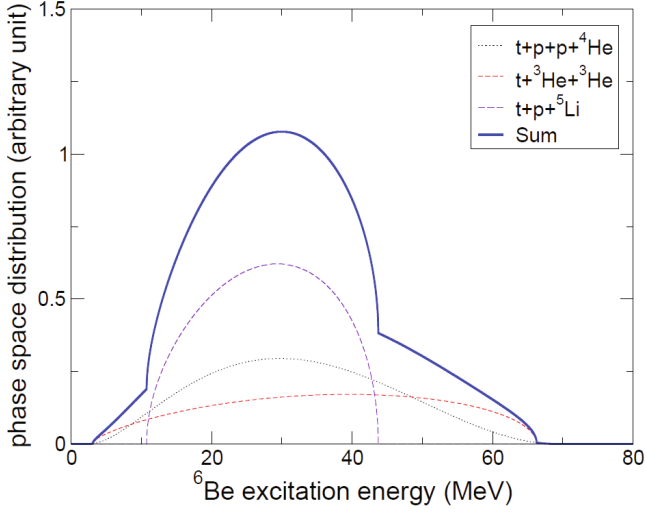


Fig. 2. (Color online) The phase space distributions for three cases at $\theta_{lab} = 13.6^\circ$.

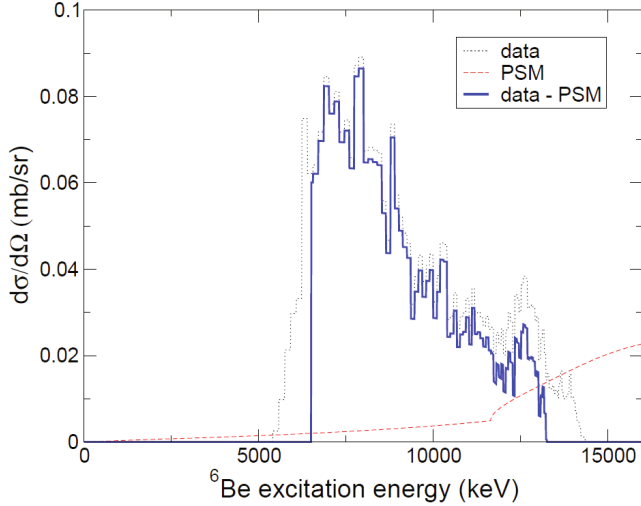


Fig. 3. (Color online) The experimental cross-section data and the PSM spectrum with proper normalization factor are shown. The blue curve shows the difference between the two sets (experimental data - PSM spectrum). $\theta_{lab} = 13.6^\circ$ in this case.

for the three exit channels are shown in Fig. 2. The total distribution, the sum of the three individual distributions, is also shown as a function of the ${}^6\text{Be}$ excitation energy.

Because the overall normalization factors of the total PSM distributions need to be determined, a free parameter C was introduced. The parameter kept being increased until the PSM distributions exceeded the experimental data. The normalized PSM distributions were

then subtracted from the measured ${}^2\text{H}({}^7\text{Be}, {}^3\text{H}){}^6\text{Be}$ reaction data at each angle. One of the results obtained at $\theta_{lab} = 13.6^\circ$ is shown in Fig. 3. The black dotted curve represents experimental data, the red dashed curve shows the PSM distribution with a proper normalization factor, and the blue solid line is the difference between the two sets. As shown in the figure, however, the overall PSM distribution is rather featureless in this energy range.

Clearly, there is very little contribution to our spectra from the phase-space decay model. As shown in Figs. 2 and 3, the PSM distribution is quite flat up to ~ 12 MeV in ${}^6\text{Be}$ excitation energy. The only big change occurs at around 12 MeV where the ${}^7\text{Be} + d \rightarrow t + p + {}^5\text{Li}$ channel starts to be effective. The peak-like structure located around 12.5 MeV in Fig. 3, however, comes from the ${}^3\text{He}$ particles that punched through the “veto” detector.

Even with the PSM distributions taken into account, no resonance in the ${}^6\text{Be}$ nucleus was evident. This does not prove that no resonance is present in the unbound ${}^6\text{Be}$ nucleus, of course, because there might be other reaction mechanisms that should be considered. The three-body continuum (sequential decay) distribution is an example. In a following work, the three-body continuum mechanism will be studied to better understand the experimentally-obtained ${}^7\text{Be}(d, t){}^6\text{Be}$ reaction cross-sections.

ACKNOWLEDGMENTS

This work was supported by a National Research Foundation of Korea (NRF) grant funded by the Korea government Ministry of Education, Science, and Technology (MEST, No. NRF-2012R1A1A1041763).

REFERENCES

- [1] K. Y. Chae *et al.*, J. Korean Phys. Soc. **61**, 1786 (2012).
- [2] E. Fermi, Prog. Theor. Phys. **5**, 570 (1950).
- [3] H. G. Bohlen, H. Ossenbrink, H. Lettau and W. Oertzen, Z. Phys. A **320**, 237 (1985).
- [4] H. G. Bohlen *et al.*, Phys. Rev. C **64**, 024312 (2001).
- [5] K. Y. Chae, *Interference effects among $J^\pi = 3/2^+$ resonances in ${}^{19}\text{Ne}$ system & Searching for resonances in the unbound ${}^6\text{Be}$ nucleus*, Ph.D. dissertation, University of Tennessee at Knoxville, 2006.
- [6] S. Nouri, Phys. Rev. A **57**, 1526 (1998).
- [7] T. Delbar, G. Gregoire, P. Belery and G. Paic, Phys. Rev. C **27**, 1876 (1983).
- [8] ENDF-6 formats manual.